Dispersion relation and growth in a free-electron laser with ion-channel guiding

Pallavi Jha* and Punit Kumar
Department of Physics, University of Lucknow, Lucknow 226007, India
(Received 18 August 1997)

A theory of a helical wiggler free-electron laser with ion-channel guiding is presented. Electron motion has been analyzed using single particle dynamics and regimes of orbit stability have been discussed. With the help of these trajectories, source currents have been obtained and the linear dispersion equation showing coupling of electromagnetic and space-charge waves by the wiggler field has been set up for a monoenergetic electron beam. Growth rates have been obtained for different ion-channel frequencies. The variation of resonant frequencies and peak growth rates with ion-channel frequency has been illustrated. Substantial enhancement in peak growth rate is obtained as the ion-channel frequency approaches the wiggler frequency. [S1063-651X(98)10901-7]

PACS number(s): 41.60.Cr, 52.75.Ms

I. INTRODUCTION

In a free-electron laser, focusing is applied to collimate the intense electron beam in the transverse direction. Focusing also enhances the growth rate by exploiting the resonance between the frequency of the focusing device and the frequency of the wiggler field. The technique of ion-channel guiding of an electron beam in a free-electron laser (FEL) has become an area of great interest, as it eliminates the need for conventional quadrupole or solenoid focusing magnets, thereby reducing the capital and running cost [1]. The presence of the ion channel allows beam currents higher than the vacuum limit and also helps radiation guiding [2]. Caporaso *et al.* [3] have shown the successful transportation of a 10 kA electron beam through the advanced test accelerator (ATA) by replacing the solenoidal guide field by an ion channel. This is effective in suppressing the transverse beam breakup (BBU) instability, which is the most serious obstacle to high current beam transport. Motivated by the need for stable transport of a multiampere beam over large distances in the FEL two beam accelerator (TBA), ion focusing has been applied in an X-band FEL experiment [4]. Chen *et al.* [5] have proposed to take advantage of continuous focusing in the ion-focused regime for application in a TeV linear electron-positron collider. Simulation studies have shown that effective gain enhancements can be obtained by introducing ion-channel guiding in FEL [6].

In ion-channel focusing, a relativistic electron beam is injected into a pre-ionized plasma channel of uniform density in the ion-focused regime (IFR) [7]. The interaction results in the formation of a positive ion core by expelling the plasma electrons along the beam. This positive ion core attracts and confines the beam electrons. The plasma channel width is of the order of the equilibrium beam radius, which helps in damping the routine instabilities that arise in transport [8]. Also the effects of emittance growth due to scattering have been found to be negligible over a wide range of parameters relevant to present day beam propagation experiments [9]. In a recent study of a helical wiggler FEL with ion-channel guiding, it has been shown that in the low-gain-per-pass limit, substantial gain enhancements are obtained under appropriate conditions [10]. This motivates the study of dispersion characteristics and consequent growth rates (not reported in literature) for such a configuration, in the high gain regime.

The purpose of the present work is to examine the FEL mechanism in the presence of the ion channel and to obtain the dispersion relation and growth rate for helical wiggler FEL. Section II deals with electron trajectories in a helical wiggler FEL with ion-channel focusing, using single particle dynamics. Regimes of stability of the electron orbit have been discussed. In Sec. III the dispersion relation showing the coupling of electromagnetic and space-charge waves by the wiggler field is derived and analyzed with the help of illustrations. Section IV is devoted to a summary and discussion of results.

II. ELECTRON MOTION

Consider a relativistic electron (charge $-e$, rest mass m, relativistic factor γ_0, energy $\gamma_0 mc^2$) moving with velocity $\vec{v}$ $(=\vec{\beta}c)$ along the z axis of a helically polarized wiggler magnetic field of amplitude B_w and wave number k_w $(=2\pi/\lambda_w)$ described by

$$\vec{B}_w = B_w(\cos k_w z, \sin k_w z, 0) \tag{1}$$

in the presence of a pre-ionized plasma channel (of uniform density) having its axis coincident with the wiggler axis. The transverse electrostatic field generated by the ion channel can be written as [7]

$$\vec{E}_i = A_i(x, y, 0), \tag{2}$$

where $A_i = 2\pi e n_i$ and n_i is the density of positive ions having charge e. With the appropriate choice of ion channel and electron beam parameters, IFR propagation may be achieved, leading to the suppression of routine instabilities that arise in beam transport. Thus in the presence of the wiggler and ion

*Author to whom correspondence should be addressed. Mailing address: 2 Faizabad Road, Lucknow 226007, India.

fields alone, the energy of the electron (or γ_0) may be considered to be a constant of motion.

The equations of motion of the electron can be written as

$$\frac{d(\gamma_0 m v_{x0})}{dt} = -eA_i x_0 + \frac{e v_{z0} B_w}{c} \sin k_w z_0, \tag{3}$$

$$\frac{d(\gamma_0 m v_{y0})}{dt} = -eA_i y_0 - \frac{e v_{z0} B_w}{c} \cos k_w z_0, \tag{4}$$

$$\frac{d(\gamma_0 m v_{z0})}{dt} = -\frac{e}{c}(v_{x0} B_w \sin k_w z_0 - v_{y0} B_w \cos k_w z_0). \tag{5}$$

Steady-state transverse electron displacements for constant axial velocity ($v_{z0}=c\beta_{z0}$; $z_0=\beta_{z0}ct$) are obtained by solving Eqs. (3) and (4);

$$x_0 = \frac{K_i c}{\gamma_0 \beta_{z0} \omega_w} \sin k_w z_0, \tag{6}$$

$$y_0 = -\frac{K_i c}{\gamma_0 \beta_{z0} \omega_w} \cos k_w z_0, \tag{7}$$

where $K_i = eB_w \beta_{z0}^2 \omega_w / mc(\omega_i^2 - \omega_w^2 \beta_{z0}^2)$ and $\omega_i^2 = 2\pi e^2 n_i / \gamma_0 m$. Hence the electron trajectory is a perfect helix (with its axis coincident with the FEL axis) characterized by transverse velocities,

$$\beta_{x0} = \frac{K_i}{\gamma_0} \cos k_w z_0, \tag{8}$$

$$\beta_{y0} = \frac{K_i}{\gamma_0} \sin k_w z_0. \tag{9}$$

These velocities are related to the axial velocity β_{z0} through

$$\gamma_0^{-2} = 1 - \beta_{x0}^2 - \beta_{y0}^2 - \beta_{z0}^2. \tag{10}$$

Equation (10) is cubic in β_{z0}^2 and describes three classes of trajectories propagating along the positive z axis of the FEL. The stability of these trajectories has been discussed in detail in Ref. [10]. A plot for β_{z0} against x $(=\omega_i/\omega_w)$ is shown in Fig. 1 for $K(=eB_w/mc\omega_w)=0.2$ and $\gamma_0=6.0$. It may be seen that three real values of axial velocity exist in regime I ($\omega_i/\omega_w<1$), whereas in regime II ($\omega_i/\omega_w>1$) only one value of β_{z0} is possible. Branches A and C are stable, while branch B is unstable. The critical value of ω_i/ω_w up to which branch A (in regime I) is stable is found to be 0.884 for the parameters used in Fig. 1. It may be noted that a circular wiggler FEL having an axial magnetic guide field also generates a similar set of stable and unstable electron orbits [11–13].

III. DISPERSION RELATION

The dispersion equation for a cold monoenergetic electron beam is obtained by solving the Lorentz force equation

$$\frac{d\vec{V}}{dt} = -\frac{e}{\gamma m}\left[\vec{E} + \frac{\vec{V}}{c}\times\vec{B} - \frac{\vec{V}}{c^2}(\vec{V}\cdot\vec{E})\right] \tag{11}$$

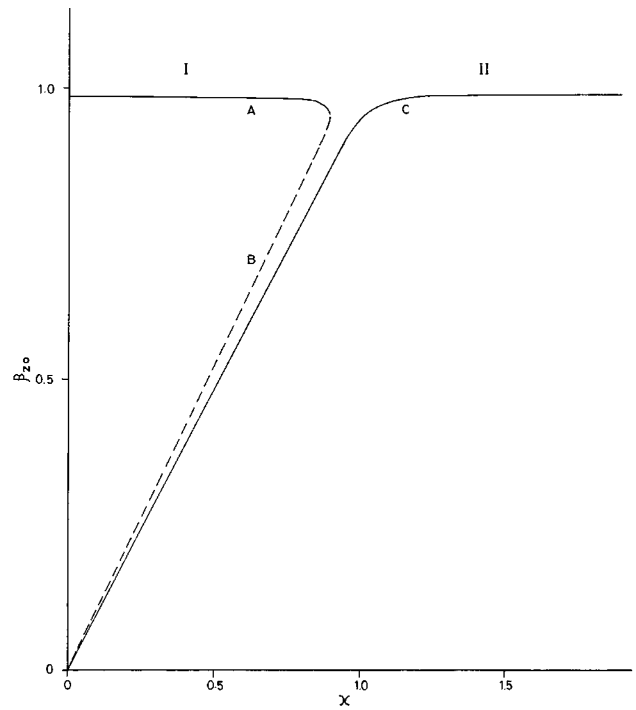

FIG. 1. Real positive values of β_{z0} versus x for $\gamma_0=6$ and $K=0.2$.

along with the equation of continuity

$$\vec{\nabla}\cdot(N\vec{V}) + \frac{\partial N}{\partial t} = 0 \tag{12}$$

and the wave equation

$$\vec{\nabla}\times(\vec{\nabla}\times\vec{E}) + \frac{1}{c^2}\frac{\partial^2 \vec{E}}{\partial t^2} + \frac{4\pi}{c^2}\frac{\partial \vec{J}}{\partial t} = \vec{0}, \tag{13}$$

where $\vec{V}$ $(=\vec{v}_0+\vec{v})$ is the sum of steady state and perturbed components of particle velocity; N $(=n_0+n)$ is the sum of the steady state and oscillatory components of the particle density; $\vec{J}$ $(=-e(n_0+n)(\vec{v}_0+\vec{v}))$ is the total current density and γ $(=[1-(|\vec{v}_0+\vec{v}|/c)^2]^{-1/2})$ is the relativistic factor. $\vec{E}$ $(=\vec{E}_r+\vec{E}_i+\vec{E}_l)$ and $\vec{B}(=\vec{B}_w+\vec{B}_r)$ are total electric and magnetic fields, respectively. The subscripts r, ω, i, and l refer to radiation, wiggler, ion channel, and space-charge fields, respectively.

The dispersion equation is obtained by linearizing Eqs. (11)–(13) and with the help of Floquet's theorem, allowing the axial and time dependence of all perturbed parameters to take the general form [14]

$$F = \sum_{n=-\infty}^{n=\infty} f_n \exp[i(k_n z - \omega t)], \tag{14}$$

where ω and k are radiation frequency and wave number, respectively; $k_n = k + nk_w$, $n = 0, \pm 1, \pm 2, \pm 3, \ldots$. We assume all transverse oscillations to be small such that $\partial/\partial x, \partial/\partial y \ll \partial/\partial z$.

Now linearizing Eq. (11) gives

$$\left(\frac{\partial}{\partial t}+v_{z0}\frac{\partial}{\partial z}\right)v_x=-\frac{e}{\gamma_0 m}\left[E_{rx}+A_i x-\frac{1}{c}v_{z0}B_{ry}-\frac{1}{c}v_z B_{wy}-\frac{1}{c^2}v_{x0}v_{z0}E_l\right]+\frac{e\gamma_0}{mc^2}\left[A_i x_0 v_{z0}v_z-\frac{1}{c}v_{z0}^2 B_{wy}v_z\right], \quad (15)$$

$$\left(\frac{\partial}{\partial t}+v_{z0}\frac{\partial}{\partial z}\right)v_y=-\frac{e}{\gamma_0 m}\left[E_{ry}+A_i y+\frac{1}{c}v_{z0}B_{rx}+\frac{1}{c}v_z B_{wx}-\frac{1}{c^2}v_{y0}v_{z0}E_l\right]+\frac{e\gamma_0}{mc^2}\left[v_{z0}v_z A_i y_0+\frac{1}{c}v_{z0}^2 v_z B_{wx}\right], \quad (16)$$

$$\left(\frac{\partial}{\partial t}+v_{z0}\frac{\partial}{\partial z}\right)v_z=-\frac{e}{\gamma_0 m}\Bigg[E_l+\frac{1}{c}v_{x0}B_{ry}+\frac{1}{c}v_x B_{wy}-\frac{1}{c}v_{y0}B_{rx}-\frac{1}{c}v_y B_{wx}-\frac{1}{c^2}(v_{z0}v_{x0}E_{rx}+v_{z0}v_{x0}A_i x+v_{z0}v_x A_i x_0$$
$$+v_{z0}v_{y0}E_{ry}+v_{z0}v_{y0}A_i y+v_{z0}v_y A_i y_0+v_{z0}^2 E_l)\Bigg], \quad (17)$$

where

$$\gamma \simeq \gamma_0\left(1+\gamma_0^2\frac{\vec{v}_0\cdot\vec{v}}{c^2}\right).$$

Substituting Eq. (14) in Eqs. (15), (16), and (17) and using orthogonality relation

$$\int_0^{\lambda_w}\exp(ik_n z)\exp(-ik_m z)\,dz=\begin{cases}0, & n\neq m\\ \lambda_w, & n=m\end{cases} \quad (18)$$

gives the expression for perturbed velocities as follows:

$$v_{xn}=-\frac{ie}{\gamma_0 m\Omega_n}\left[E_{xn}+A_i x_n-\beta_{z0}B_{yn}-\frac{K_i\beta_{z0}}{2\gamma_0}(E_{ln-1}+E_{ln+1})\right]+\frac{e\gamma_0}{2mc\Omega_n}\left[B_w\left(\frac{1}{\gamma_0^2}-\beta_{z0}^2\right)+\frac{K_i A_i c}{\gamma_0\omega_w}\right](v_{zn-1}-v_{zn+1}), \quad (19)$$

$$v_{yn}=-\frac{ie}{\gamma_0 m\Omega_n}\left[E_{yn}+A_i y_n+\beta_{z0}B_{xn}-\frac{K_i\beta_{z0}}{2i\gamma_0}(E_{ln-1}-E_{ln+1})\right]-\frac{ie\gamma_0}{2mc\Omega_n}\left[B_w\left(\frac{1}{\gamma_0^2}-\beta_{z0}^2\right)+\frac{K_i A_i c}{\gamma_0\omega_w}\right](v_{zn-1}+v_{zn+1}), \quad (20)$$

$$v_{zn}=-\frac{ie}{\gamma_0 m\Omega_n}\Bigg[\frac{K_i}{2\gamma_0}(B_{yn-1}+B_{yn+1})+\left(\frac{B_w}{2ic}-\frac{K_i A_i}{2i\gamma_0\omega_w}\right)(v_{xn-1}-v_{xn+1})-\frac{K_i}{2i\gamma_0}(B_{xn-1}-B_{xn+1})$$
$$-\left(\frac{B_w}{2c}-\frac{K_i A_i}{2\gamma_0\omega_w}\right)(v_{yn-1}+v_{yn+1})-\frac{K_i\beta_{z0}}{2\gamma_0}(E_{xn-1}+E_{xn+1})-\frac{K_i\beta_{z0}A_i}{2\gamma_0}(x_{n-1}+x_{n+1})-\frac{K_i\beta_{z0}}{2i\gamma_0}(E_{yn-1}-E_{yn+1})$$
$$-\frac{K_i A_i\beta_{z0}}{2i\gamma_0}(y_{n-1}-y_{n+1})+\frac{E_{ln}}{\gamma_{z0}^2}\Bigg], \quad (21)$$

where $\Omega_n=\omega-k_n v_{z0}$ and $\gamma_{z0}^{-2}=(1-\beta_{z0}^2)$. Using Maxwell's equation $\vec{\nabla}\times\vec{E}+(1/c)(\partial\vec{B}/\partial t)=0$ and applying orthogonality condition [Eq. (18)] give $B_{xn}=-(ck_n/\omega)E_{yn}$ and $B_{yn}=(ck_n/\omega)E_{xn}$. Retaining terms up to second order in wiggler magnetic field, Eqs. (19), (20), and (21) reduce to

$$v_{xn}=-\frac{ie}{\gamma_0 m\Omega_n\Omega_{in}}\left[1-\frac{\beta_{z0}k_n c}{\omega}\right]E_{xn}, \quad (22)$$

$$v_{yn}=-\frac{ie}{\gamma_0 m\Omega_n\Omega_{in}}\left[1-\frac{\beta_{z0}k_n c}{\omega}\right]E_{yn}, \quad (23)$$

$$v_{zn}=-\frac{ie}{\gamma_0 m\Omega_n}\Bigg[(A-B)E_{xn-1}+(C+D)E_{xn+1}$$
$$+\frac{1}{i}[(A-B)E_{yn-1}-(C+D)E_{yn+1}]+\frac{E_{ln}}{\gamma_{z0}^2}\Bigg], \quad (24)$$

where

$$\Omega_{in}=\left(1-\frac{\omega_i^2}{\Omega_n^2}\right),$$

$$A=\frac{K_i c}{2\gamma_0}\left(\frac{k_{n-1}}{\omega}-\frac{\beta_{z0}}{c}\right),$$

$$B=\frac{e}{2mc\gamma_0\Omega_{n-1}\Omega_{in-1}}\left[B_w+\frac{K_iA_i\beta_{z0}c}{\gamma_0}\left(\frac{1}{\Omega_{n-1}}-\frac{1}{\omega_w\beta_{z0}}\right)\right]\times\left(1-\frac{c\beta_{z0}k_{n-1}}{\omega}\right),$$

$$C=\frac{K_i c}{2\gamma_0}\left(\frac{k_{n+1}}{\omega}-\frac{\beta_{z0}}{c}\right),$$

$$D=\frac{e}{2mc\gamma_0\Omega_{n+1}\Omega_{in+1}}\left[B_w-\frac{K_iA_i\beta_{z0}c}{\gamma_0}\times\left(\frac{1}{\Omega_{n+1}}+\frac{1}{\omega_w\beta_{z0}}\right)\right]\left(1-\frac{c\beta_{z0}k_{n+1}}{\omega}\right).$$

The linearized current density, $\vec{J}=-e(n\vec{v}_0+n_0\vec{v})$ is obtained from Eqs. (12) and (14) as follows:

$$J_{xn}=-en_0v_{xn}-\frac{en_0K_ic}{2\gamma_0}\left(\frac{v_{zn-1}k_{n-1}}{\Omega_{n-1}}+\frac{v_{zn+1}k_{n+1}}{\Omega_{n+1}}\right), \tag{25}$$

$$J_{yn}=-en_0v_{yn}+\frac{ien_0K_ic}{2\gamma_0}\left(\frac{v_{zn-1}k_{n-1}}{\Omega_{n-1}}-\frac{v_{zn+1}k_{n+1}}{\Omega_{n+1}}\right), \tag{26}$$

$$J_{zn}=-\frac{en_0\omega v_{zn}}{\Omega_n}. \tag{27}$$

The dispersion equation is now obtained by substituting source currents [Eqs. (25), (26), and (27)] and perturbed velocities [Eqs. (22), (23), and (24)] into the wave equation [Eq. (13)]. Thus,

$$(\omega^2-c^2k_n^2)-\frac{\omega_b^2\omega}{\gamma_0\Omega_n\Omega_{in}}\left(1-\frac{\beta_{z0}k_nc}{\omega}\right)=\frac{\omega_b^2\omega K_ick_{n+1}}{2\gamma_0^2R_{n+1}\Omega_{n+1}^2}\left\{\frac{K_ic}{\gamma_0}\left(\frac{k_n}{\omega}-\frac{\beta_{z0}}{c}\right)-\frac{e}{\gamma_0mc\Omega_n\Omega_{in}}\left[B_w+\frac{K_iA_i\beta_{z0}c}{\gamma_0}\left(\frac{1}{\Omega_n}-\frac{1}{\omega_w\beta_{z0}}\right)\right]\left(1-\frac{c\beta_{z0}k_n}{\omega}\right)\right\}, \tag{28}$$

where $\omega_b=(4\pi n_0e^2/\gamma_0m)^{1/2}$ and $R_n=(1-\omega_b^2/\Omega_n^2\gamma_{z0}^2)$. Equation (28) describes the dispersion properties of pure electromagnetic modes in combined wiggler and ion-channel fields. For the lowest mode, $n=0$ and upshifted frequencies $\omega\simeq(k+k_w)v_{z0}$ this equation reduces to the sought-after dispersion equation

$$\left[(\omega^2-c^2k^2)-\frac{\omega_b^2(\omega-kv_{z0})^2}{\gamma_0[(\omega-kv_{z0})^2-\omega_i^2]}\right]\left[[\omega-(k+k_w)v_{z0}]^2-\frac{\omega_b^2}{\gamma_0\gamma_{z0}^2}\right]=\frac{\omega_b^2\omega}{2\gamma_0^2}(k+k_w)K_ic\left[\frac{K_ic}{\gamma_0}\left(\frac{k}{\omega}-\frac{\beta_{z0}}{c}\right)-\left[K\omega_w+\frac{K_i\omega_i^2}{\omega_w}\left(\frac{\omega_w\beta_{z0}}{(\omega-kv_{z0})}-1\right)\right]\frac{(\omega-kv_{z0})^2}{\omega\gamma_0[(\omega-kv_{z0})^2-\omega_i^2]}\right]. \tag{29}$$

This equation describes the coupling between the electrostatic beam mode with the electromagnetic modes. In the absence of the ion channel ($\omega_i=0$), Eq. (29) reduces to the well known FEL dispersion relation [15]. The sixth-order equation in k [Eq. (29)] has been solved on a computer. For a wiggler field of wavelength $\lambda_w=3$ cm, growth rates (Im k) are plotted versus frequency for appropriate values of x $(=\omega_i/\omega_w)$ for regimes I and II in Figs. 2 and 3, respectively. For these values of x the electron trajectories are stable as is evident from Fig. 1. Different values of electron beam frequency ($\omega_b=1.8\times10^{11}\ \mathrm{sec}^{-1}$ and $4.4\times10^{11}\ \mathrm{sec}^{-1}$, respectively) for regimes I and II have been chosen so as to satisfy the Budker condition ($n_0>n_i\gg n_0/\gamma_0^2$) [16] for propagation of an electron beam in IFR. It may be seen that for each value of x, the growth rate initially increases, attains a maximum value, and then decreases to zero. Peak growth rate is found to occur for $\omega\simeq(1-\beta_{z0})^{-1}k_wv_{z0}$, which corresponds to the well-known free-electron laser condition. In Fig. 2 it is seen that as x increases, the resonant frequency decreases, whereas in contrast Fig. 3 shows that in regime II, increase in x leads to a slight increase in the value of resonant frequency.

An illustration of frequency versus x is shown in Fig. 4. The resonant frequency ω ($\simeq c$ Re k) is obtained from real part of the solution of Eq. (29) at peak growth. The variation in frequency is found to be in agreement with that seen in Figs. 2 and 3. A plot of peak growth rate with x for regimes I and II (for the same parameters as in Figs. 2 and 3) is shown in Fig. 5. In regime I, with an increase in x, the peak growth rate increases monotonically up to the singularity at the orbital stability boundary ($x=0.884$ for this choice of parameters). In regime II, the peak growth rate decreases slowly as ω_i becomes large. This behavior is in qualitative agreement with that found previously in the context of low gain theory [10]. The variations in frequency and growth rate are also qualitatively similar to those obtained with an axial magnetic guiding field in a circular wiggler FEL [17–20]. Thus it may be concluded that growth rate enhances as the frequency of the focusing device approaches the frequency of the wiggler.

IV. SUMMARY AND DISCUSSION

In this paper we have analyzed the effect of ion-channel guiding on a helical wiggler FEL. Steady-state helical trajec-

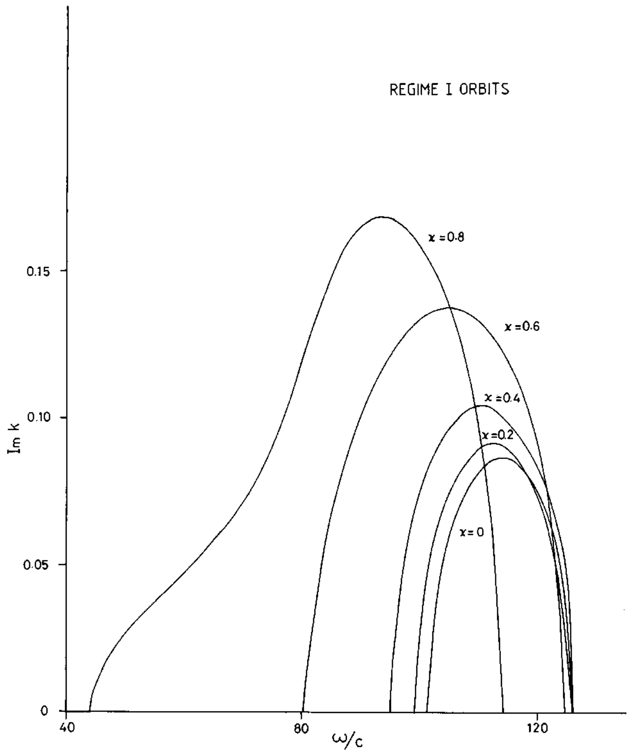

FIG. 2. Spatial growth rate Im $k\,(\mathrm{cm}^{-1})$ vs ω/c (cm^{-1}) for regime I orbits, such that $\gamma_0=6$, $K=0.2$, $\lambda_w=3$ cm, $\omega_b=1.8\times10^{11}\ \mathrm{sec}^{-1}$.

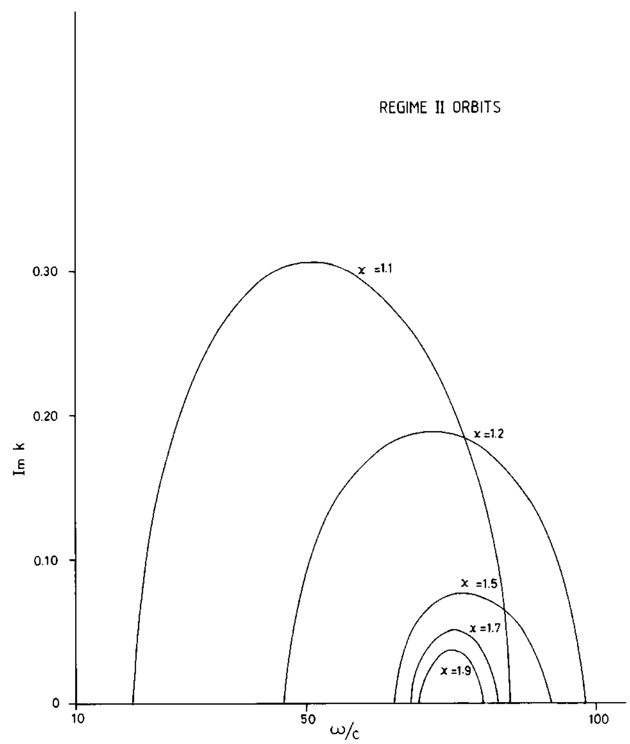

FIG. 3. Spatial growth rate Im $k\,(\mathrm{cm}^{-1})$ vs ω/c (cm^{-1}) for regime II orbits, such that $\gamma_0=6$, $K=0.2$, $\lambda_w=3$ cm, $\omega_b=4.4\times10^{11}\ \mathrm{sec}^{-1}$.

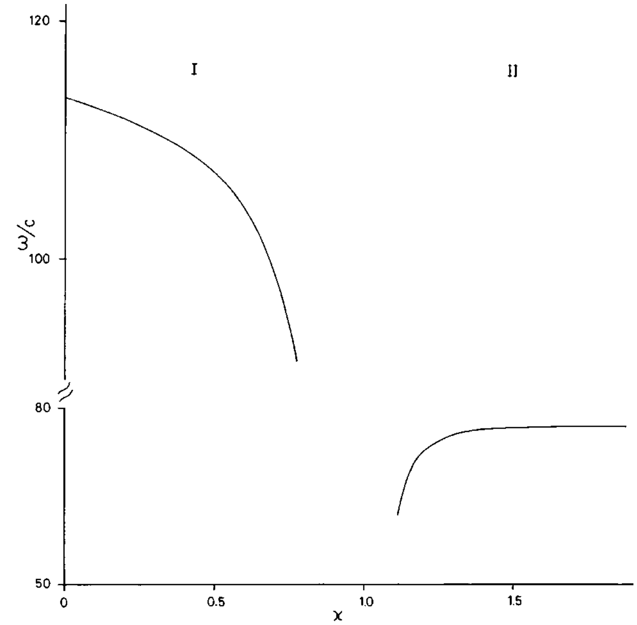

FIG. 4. Graph of ω/c (cm^{-1}) as a function of x for regimes I and II.

tories of the electron have been obtained using single particle dynamics. Illustration for $\gamma_0=6$ and $K=0.2$ has been shown and regimes of orbit stability have been identified. With the help of these single particle trajectories the fluctuating source currents are obtained and a linearized dispersion relation for electron-radiation interaction has been set up. It is found that with $x(=\omega_i/\omega_w)=0$ this relation reduces to that obtained for a helical wiggler FEL in the absence of ion-channel guiding. The sixth-order dispersion equation in k has been solved

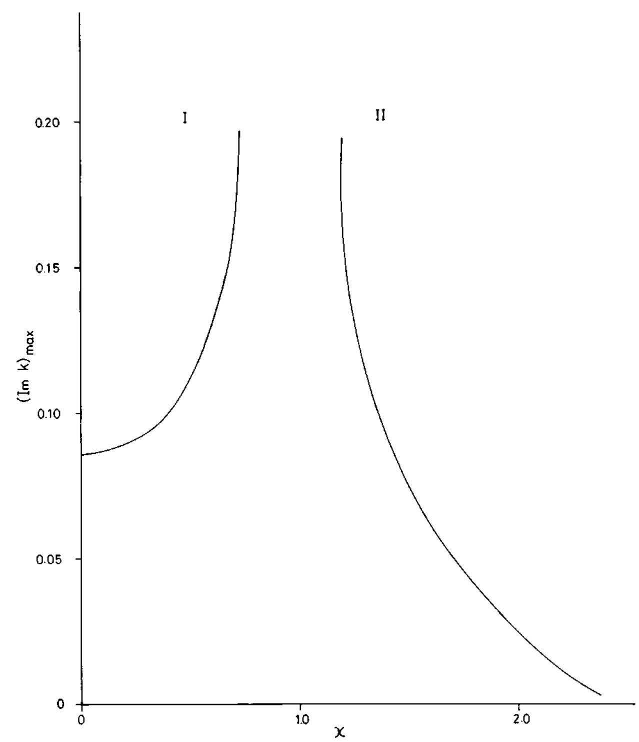

FIG. 5. Peak growth rate $(\mathrm{Im}\ k)_{\max}$ (cm^{-1}) as a function of x for regimes I and II.

with the help of a computer and the linearized growth rates (Im k) have been obtained for different values of x. Plots showing the variation of growth rate with radiation frequency, for various values of normalized ion-channel frequencies, are given. The shift of resonant frequency with change in x has also been illustrated and is found to be in agreement with the values of resonant frequencies at which peak growth rates occur in Figs. 2 and 3. The effect of ion channel on peak growth rate is shown in Fig. 5. It may be noted that the presence of ion-channel focusing leads to substantial enhancements in growth rate as the ion-channel frequency approaches the frequency of the wiggler field. This is found to be in qualitative agreement with results obtained earlier in the low gain regime.

[1] K. Takayama and S. Hiramatsu, Phys. Rev. A **37**, 173 (1988).

[2] Y. Seo, V. K. Tripathi, and C. S. Liu, Phys. Fluids B **1**, 221 (1989).

[3] G. J. Caporaso, F. Rainer, W. E. Martin, D. S. Prono, and A. G. Cole, Phys. Rev. Lett. **57**, 1591 (1986).

[4] T. Ozaki, K. Ebihara, S. Hiramatsu, Y. Kimura, J. Kishuro, T. Monaka, K. Takayama, and D. H. Whittum, Nucl. Instrum. Methods Phys. Res. A **318**, 101 (1992).

[5] P. Chen, K. Oide, A. M. Sessler, and S. S. Yu, Phys. Rev. Lett. **64**, 1231 (1990).

[6] P. Jha and J. S. Wurtele, Nucl. Instrum. Methods Phys. Res. A **331**, 477 (1993).

[7] D. H. Whittum, Ph.D. dissertation, University of California at Berkeley (1990), Chap. 2.

[8] D. H. Whittum, Phys. Fluids B **4**, 730 (1992).

[9] T. P. Hughes and B. B. Godfrey, Phys. Fluids **27**, 1531 (1984).

[10] P. Jha and P. Kumar, IEEE Trans. Plasma Sci. **24**, 1359 (1996).

[11] R. C. Davidson and H. S. Uhm, Phys. Fluids **23**, 2076 (1980).

[12] L. Friedland, Phys. Fluids **23**, 2376 (1980).

[13] H. F. Freund and A. T. Drobot, Phys. Fluids **25**, 736 (1983).

[14] Y. Z. Yin and G. Bekefi, J. Appl. Phys. **55**, 33 (1984).

[15] C. W. Roberson and P. Sprangle, Phys. Fluids B **1**, 3 (1989).

[16] G. J. Budker (unpublished).

[17] H. P. Freund, P. Sprangle, D. Dillenburg, E. H. da Jornada, B. Liberman, and R. S. Schneider, Phys. Rev. A **24**, 1965 (1981); Phys. Rev. A **26**, 2004 (1982).

[18] L. Friedland and A. Fruchtman, Phys. Rev. A **25**, 2693 (1982).

[19] H. P. Freund, Phys. Rev. A **27**, 1977 (1983).

[20] T. P. Pandya, L. M. Bali, U. Bakshi, and P. Jha, Phys. Rev. A **35**, 5131 (1987).